aircraft is dry washed or polished. Total lapse time is approximately six hours. This accomplishment is credited to the specialized equipment for gaining easy and rapid access to all areas of the exterior surface.

Several operators are evaluating a barrier coating over the areas of high soil exposure. This coating traps the soils on the surface without permitting them to embed in the paint. At the washing cycle, the barrier coating is released from the airplane surface by a chemical solution which is spray applied. With the release of the barrier coating, the soils are removed, leaving the regular painted surface fairly easy to clean by the conventional cleaning materials and methods. The barrier coating is then reapplied.

Another two operators are reported to be flight testing a clear polyurethane topcoating which is applied over glossy, pigmented paint. Purpose of the test is to determine if the topcoat will prolong gloss retention of the pigmented surface and if it will enhance cleaning time and effort.

The Military Aircraft Command is planning indoor facilities for complete washing of its C-5A fleet. Outdoor facilities will continue to be used, but hopefully limited to the washing of lower surfaces which are accessible from portable stands and standard length brushes and mops.

Fraternal Approach Toward Alleviation

Procedural problems are surmountable for effective, efficient cleaning of jumbo jets. In time, special equipment will be developed, as will satisfactory cleaning compounds; nevertheless, much of the developments will have to be tailored to specific aircraft configurations, cleaning locations, schedule requirements, and operational spectrum. For resolutions to the procedural problems for washing mammoth aircraft, contributions must be applied willingly from the experiences of aircraft manufacturers, operators, washing contractors, and the specialized chemical compounders. Testing and evaluating of special products and equipment are of interest to all operators; consequently, a mutual organization should have this information for assessing materials and procedures and for recommending improvements. Such an organization is the Air Transport Association, which has an active committee for aircraft cleaning. This committee has both civil and military participation. By the active participation of its members, uniformity of procedures will be promoted so that economy can be shared by all contributors. By collective action of concerned and technically capable people, the procedural problem of washing the jumbo jet will be resolved.

Performance of an Inlet for an Integrated Scramjet Concept

Carl A. Trexler*
NASA Langley Research Center, Hampton, Va.

Introduction

DURING the past decade, the USAF and NASA have funded the development of several small-scale research scramjet engines. These projects have shown that the scramjet is a feasible engine concept; practical levels of thrust have been demonstrated and a substantial technology base has been established.[1] NASA is now conducting a hypersonic (Research and Testing) program[2,3] which is devoted in part to the next logical step in scramjet evolution, the development of engine concepts which will integrate with the airframe. Integration includes the use of the vehicle forebody to precompress the engine airflow before it enters the inlet and the use of the vehicle afterbody for additional expansion of the nozzle exhaust gas. Other principal design criteria are low engine cooling requirements to make part of the heat sink of the hydrogen fuel available for active cooling of the airframe, fixed geometry to reduce weight and system complexity, and minimum external drag. Detailed design studies utilizing advanced basic technology have resulted in the definition of a unique engine concept (Fig. 1 and Ref. 4), which conservative predictions indicate will meet all the above design objectives. Innovative design features of the inlet and combustor coupled with the favorable effects of integration permit high levels of performance over the Mach range from 4 to 10 with relatively low cooling requirements. For instance, at Mach 6 a specific impulse of about 3000 sec is predicted with only 40% of the fuel heat sink required for engine cooling. Experimental investigations are now in progress to substantiate and further develop the design concept; the present Note reports briefly on the measured performance of the inlet at Mach 6.

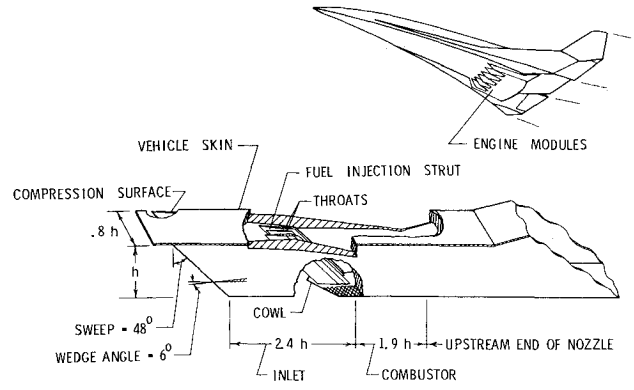

Fig. 1 Inner module of Langley Scramjet Module Concept.[4]

Inlet Design Concept

The cross section of the Langley Scramjet module (Fig. 1) varies from a nearly square capture area to a rectangular inlet throat to a square combustor exit. This type of configuration favors low cooling requirements by reducing the internal wetted area. In addition, a cluster of several such modules mounted on the underside of the vehicle is capable of capturing all the airflow lying between the vehicle surface and the vehicle bow shock at the maximum Mach number, thus producing a maximum thrust. Wall fuel injectors would produce very long mixing lengths for this configuration; therefore, three fuel injection struts have been provided to allow six planes of fuel injection in the stream. This feature not only shortens the combustor but also the inlet since the struts provide a significant part of the inlet flow compression. The leading edges of the sidewalls and all downstream stations are swept at 48° to provide spillage at low Mach numbers for starting with fixed geometry. Spillage occurs through the open window upstream of the cowl leading edge, which is bathed by shocks from the sidewall compression surfaces. The combination of the sweep angle, the sidewall design, and the cowl leading edge location produces near-maximum mass capture ratios as a function of Mach number, and the spilled flow provides a lift increment for the vehicle. The

Received April 15, 1974.
Index categories: Airbreathing Propulsion; Hypersonic.
*Aerospace Technologist, Hypersonic Vehicles Division, Advanced Concepts Section.

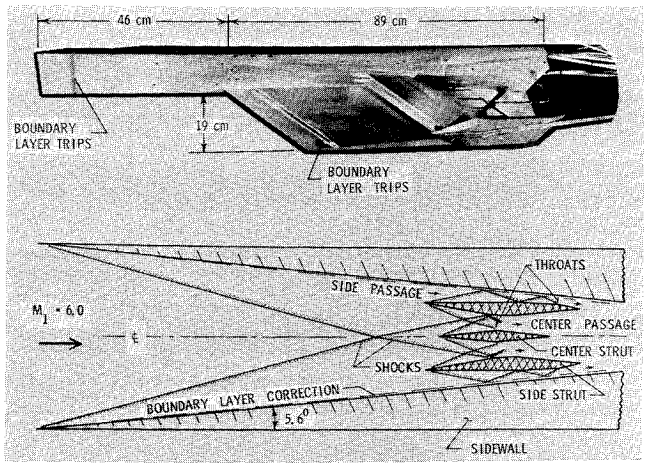

Fig. 2 Inlet model and Mach 6 shock diagram.

swept shock system also provides less compression near the vehicle underbody and allows the inlet to ingest the vehicle forebody boundary layer without separation. The external surface of the cowl is parallel to the local body line of the vehicle and has a very small drag.

The photograph in Fig. 2 shows one inlet sidewall removed and a rake used to measure captured mass flow. The top plate generates a boundary layer similar to that on a vehicle forebody. The boundary-layer trips were steel balls with a 0.16 cm diam. Pitot and static pressure surveys were made at several vertical locations in the throats of the side and center passages (Figs. 2 and 3) and at the mass flow station; 102 static pressure orifices were distributed throughout the model.

Mach 6 Experimental Results

The swept geometry inlet started easily at Mach 6 and subsequent, recent data indicates enough spillage is provided for starting below Mach 2.5. The Mach 6, theoretical shock diagram in a horizontal plane was verified ex-

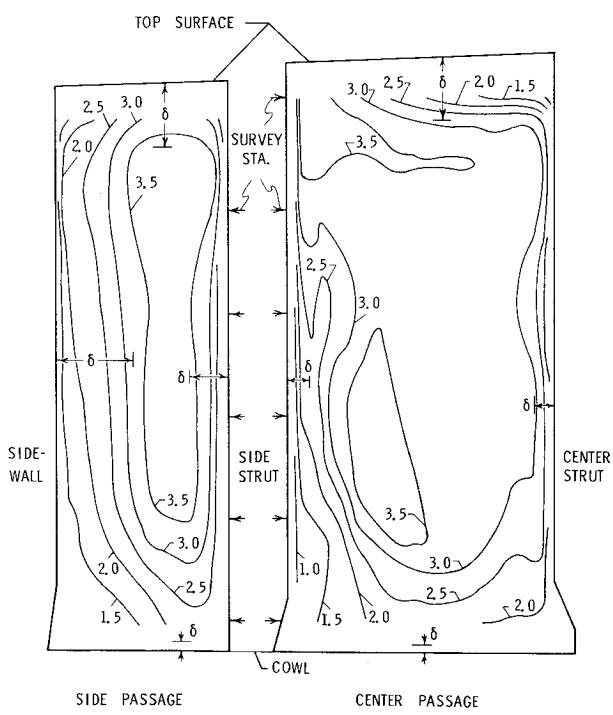

Fig. 3 Throat Mach number contours, mass weighted M = 3.0 (not to scale).

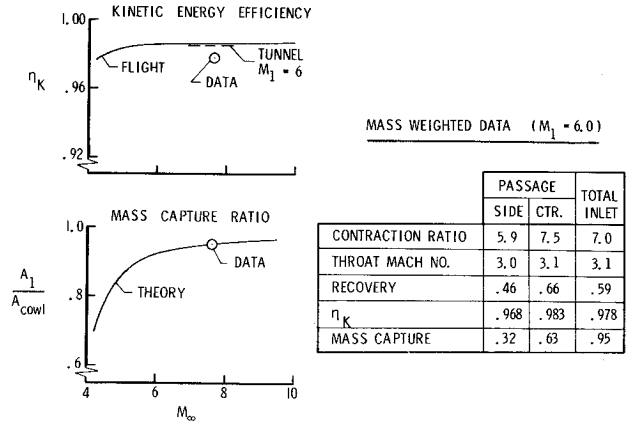

	PASSAGE		TOTAL INLET
	SIDE	CTR.	
CONTRACTION RATIO	5.9	7.5	7.0
THROAT MACH NO.	3.0	3.1	3.1
RECOVERY	.46	.66	.59
η_K	.968	.983	.978
MASS CAPTURE	.32	.63	.95

Fig. 4 Integrated performance parameters.

perimentally; the sidewall shocks corresponded to a total turning of 6.8°, including a 1.2° boundary-layer correction. The strut portions upstream of the throats shortened the inlet by furnishing 75% of the over-all inlet compression.

The survey data were processed and analyzed by a digital computer program which by a curve-fitting interpolation procedure expanded the data into a network of approximately 1000 grid points, covering the entire throat flow area. Besides performing numerical integrations, Mach number, total pressure, and unit mass flow were calculated for each grid point; and contour maps of each parameter were plotted by the computer's graphics system. The resulting Mach number contours are given in Fig. 3 where the width scale is 7 times the height scale for both passages.

The side passage throat contours are relatively symmetrical, and the predictions of boundary-layer thickness δ agree well for the top and side surfaces. A nearly horizontal shock of about 8° turning was generated by the cowl leading edge and is still near the cowl surface at the throat. This discrete shock is smeared by the interpolation process; and consequently a vertical Mach number gradient, extending well beyond the predicted δ for the cowl, is indicated. There is some rounding of the contours at the corners, but no flow separation was detected. Note that most of the vertical walls were relieved near the cowl surface to counteract the excess compression produced by the cowl shock. The Mach number contours of the center passage are not as symmetrical due to the greater shock wave concentration, Fig. 2; however, the Mach 3 (mass weighted average) contour encloses the major portion of the total area.

Integrated parameter performance is given in Fig. 4, for Mach 6 flow in front of the inlet, which simulates a flight Mach number of 7.6. The measured mass flow capture of 95% matches the predicted curve value. The curve is slightly higher than found in Ref. 4 because the fuel injection struts and cowl have been moved upstream 4.1 cm to achieve the shock diagram of Fig. 2. The measured kinetic energy efficiency is 97.8% compared with the predicted tunnel value of 98.5%. The predicted curves are slightly high primarily because the cowl shock and viscous corner interactions were not included. The aerodynamic contraction ratio, which is based on the average throat Mach number and total pressure, is 7.0 instead of the value of 8.7 found in Ref. 4; because moving the struts upstream increased the throat width somewhat and because the measured total pressure recovery was somewhat lower. The side passage total pressure recovery was lower than the center passage recovery because of the relatively thicker boundary layers in the side passage. The strut positioning within the inlet provided a split in mass flow between the center and side passages in the ratio of 63/32.

The small differences between the experimental and predicted inlet performance will not have a significant effect on the engine thrust performance quoted in Ref. 4.

References

[1]Henry, J. R. and McLellan, C. H., "The Air-Breathing Launch Vehicle for Earth-Orbit Shuttle—New Technology and Development Approach," *Journal of Aircraft*, Vol. 8, No. 5, May 1971, pp. 381–387.

[2]Becker, J. V., "New Approaches to Hypersonic Aircraft." Presented at the 7th Congress of the International Council of the Aeronautical Sciences, Rome, Italy, Sept. 1970; also Becker, J. V., "Prospects for Actively Cooled Hypersonic Transports," *Astronautics & Aeronautics*, Vol. 9, No. 8, Aug. 1971, pp. 32–39.

[3]Brown, D. A. et al., "Development of Liquid-Hydrogen Scramjet Key to Hypersonic Flight," *Aviation Week and Space Technology*, Sept. 17, 1973, pp. 75–78.

[4]Henry, J. R. and Anderson, G. Y., "Design Considerations for the Airframe-Integrated Scramjet," TM X-2895, 1973, NASA.

Influence of Flaps and Engines on Aircraft Wake Vortices

David C. Burnham* and Thomas E. Sullivan†
U.S. Department of Transportation, Transportation Systems Center, Cambridge, Mass.

ALTHOUGH previous investigations have shown that the nature of aircraft wake vortices depends on the aircraft type and flap configuration, the causes for these differences have not been clearly identified. In this Note we show that observed differences in vortex core structure are related to engine placement, engine thrust and wing flap deflection angle.

Much of the quantitative information on the velocity distribution within aircraft vortices has been collected by the Federal Aviation Administration's National Aviation Facilities Experimental Center (NAFEC) in Atlantic City, N.J. In these experiments (conducted at NAFEC and Idaho Falls, Idaho) flight paths of test aircraft were selected so the vortices would drift through an instrumented smoke tower. Hot wire anemometers were used to measure vortex velocities. Smoke grenades placed at regular intervals on the tower provided flow visualization of the vortex. These tests have shown that most vortices can be divided into two general classes:[1]

1) Tubular (T): The vortex has high tangential velocities concentrated in a very tight core. Long tubular smoke streamers can be observed along the vortex axis when such a vortex passes near a smoke grenade on the tower.

2) Nontubular (NT): The vortex has substantially lower tangential velocities and a large diffused vortex core. Little axial transport of injected smoke is observed.

The types of vortices observed in NAFEC tower tests are listed in Table 1. For all configurations, the engine thrust was adjusted to maintain level flight past the tower. The vortices from aircraft with four-wing mounted engines configured for takeoff were designated "semitubular" (somewhat larger cores than in holding configuration). Note that the only significant differences occur in landing configuration.

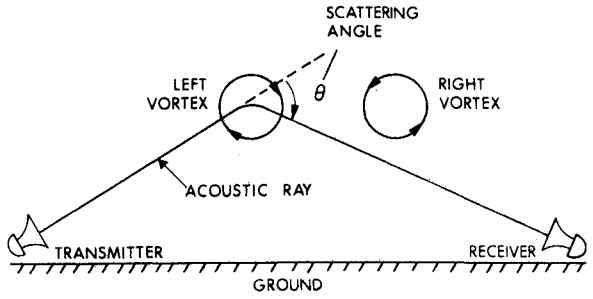

Fig. 1 Geometry for acoustic scattering from aircraft vortices.

Table 1 Vortex type[a] vs aircraft type and configuration

Aircraft type	Aircraft configuration[b] Holding	Takeoff	Landing
Propeller driven (DC-7)	T	T	T
No wing-mounted engines (B-727)	T	T	T
Four wing-mounted engines (B-707)	T	T^c	NT

[a] According to instrumented tower measurements (T = tubular, NT = nontubular).

[b] Flap extensions: Holding, none; Takeoff, partial; Landing, full.

[c] Semitubular.

An independent but consistent vortex classification can be obtained by interpreting data obtained with a pulsed bistatic acoustic vortex sensing system developed at the Transportation Systems Center.[2] In this system acoustic pulses are transmitted from one side of an aircraft flight path and received on the other. The presence of a received signal from the vortex depends on its acoustic ray-bending properties. The maximum scattering angle Θ_m (see Fig. 1) is particularly sensitive to the type of vortex core (for a given circulation, the smaller the vortex core, the larger the maximum scattering angle, Θ_m). Thus a tubular vortex would be expected to have a significantly larger value of Θ_m than a nontubular vortex. Tests conducted at several airports have shown that vortices from landing aircraft could be classified on the basis of observed Θ_m with the same results as in Table 1. Propeller driven aircraft, aircraft with no wing-mounted engines and aircraft with two wing-mounted engines (DC-10, B-737), were found to give typical values of $\Theta_m = 1.2$ rad or higher. Aircraft with four wing-mounted engines (DC-8 and B-707) typically gave values of $\Theta_m = 0.5$ rad. Intermediate values of Θ_m, which appeared to depend on the ambient wind conditions, were observed for the B-747 (four wing-mounted engines). Acoustic measurements made at NAFEC show that aircraft with four wing-mounted engines generate vortices with large scattering angles ($\Theta_m \geq 1.0$ rad) in both holding and takeoff configurations.

In order to explain the observed differences in core structure one must take into account the effect of flap angle on the origin of a vortex from an aircraft wing. In general, the vortex core is generated at the edge of the lift distribution, which in "holding" or "cruise" configuration (zero flap angle) is located at the tip. However, in landing configuration (full flaps) relatively little lift is generated by that portion of the wing beyond the outboard edge of the flaps. The vortex generated by the strong lift discontinuity at the flap edge is therefore likely to dominate the formation of the vortex core with relatively little pertur-

Received May 20, 1974. We would like to acknowledge the cooperation and assistance of NAFEC personnel and the aircraft pilots during the tower fly-by tests reported here.

Index categories: Aircraft Aerodynamics (Including Component Aerodynamics); Jets, Wakes, and Viscid-Inviscid Flow Interactions.

*Staff Scientist.

†Staff Engineer.